© smp chair committee (Kourosh Koushan and Sverre Steen)
DOI: 10.15480/882.9351

Eighth International Symposium on Marine Propulsors
smp'24, Berlin, Germany, March 2024

# An Experimental Study on Visualisation and Passive Control of Model Propeller Boundary Layers

**Bart Schuiling, Maarten Kerkvliet, Douwe Rijpkema**

Maritime Research Institute Netherlands (MARIN), Wageningen, The Netherlands

**ABSTRACT**

This paper examines the complications of a laminar propeller boundary layer during towing tank model testing and proposes a solution in the form of turbulence stimulation to improve the consistency and reliability of model testing procedures. Although common for model ships and their appendages, this approach is novel for propellers in the maritime industry. In an effort to promote widespread adoption, this paper presents two innovations.

The first is a modernised experimental method for conducting propeller paint tests to visualise the boundary layer flow. We validate this method, highlight key considerations, and provide illustrative examples for a comprehensive understanding.

The second innovation is the development of 'turbulators', a novel, low-cost and practical technique for inducing a turbulent boundary layer on model propellers. By systematically varying the height of the turbulators for a test-case propeller, it was possible to estimate their isolated effect on propeller performance. The results show that turbulators impose only a marginal penalty of 0.1% on both open water efficiency and thrust. However, the transition to a turbulent boundary layer regime resulted in a significant difference of 4.9% in efficiency and 12.9% in thrust for this particular test-case propeller.

In order to support the recommendation for the application of turbulence stimulation to model propellers, this study analysed a number of contemporary propeller designs. The methodology involved quantifying the effect of turbulence stimulation on propeller performance. In addition, the boundary layer was examined both with and without turbulence stimulation using paint tests. The comparative analysis of the different propeller types revealed varying degrees of sensitivity to low Reynolds number effects and the impact of turbulence stimulation. This sensitivity was particularly pronounced for propellers with smaller blade areas, where turbulence stimulation significantly reduced efficiency.

In summary, this research enhances the understanding of boundary layer behaviour on model propellers and suggests the use of turbulence stimulation to improve the consistency of model testing. These advancements provide the basis for more accurate predictions of full-scale performance and ultimately contribute to the development of more efficient marine propulsion systems.

**Keywords**

Model propeller, Reynolds effects, laminar-turbulence transition, flow separation, experimental boundary layer visualisation, paint test, turbulence stimulation, turbulators.

## 1 INTRODUCTION

### 1.1 Background

For over a century, towing tank testing has remained a cornerstone in the maritime industry for predicting ship performance. Despite its long-standing application, MARIN continuously seeks to improve the accuracy and reliability of experimental and extrapolation procedures for predicting ship performance. One prominent source of uncertainty in modern powering predictions through model tests is the difference in the propeller boundary layer regime when comparing model tests to the expected conditions of full-scale propellers. At the model-scale, the propeller boundary layer can exhibit laminar or transition into to turbulent flow. In contrast, the boundary layer for full-scale propellers is typically fully turbulent.

The discrepancy in propeller boundary layer between model and full-scale arises from two main factors. The first issue is the well-known challenge of Reynolds scaling, where the ratio of inertial to viscous forces at the model scale is not accurately replicated due to experimental constraints. Secondly, it was historically decided that, in contrast to ship models (Hughes & Allen 1951), applying turbulence stimulation to model propellers should be omitted during performance tests.

The fact that differences in the propeller boundary layer regime between model and full-scale ships introduce uncertainties in performance predictions is not a recent discovery. This was notably pointed out by van Lammeren (1939). His conclusions were informed by the detailed experimental studies previously conducted by Gutsche (1936). Van Lammeren cautioned against making definitive conclusions regarding scale effects from open-water propeller model tests without a thorough understanding of the boundary layer's nature. He articulated that propeller

efficiency can either increase or decrease with an increasing Reynolds number, depending on the boundary layer regime and the magnitude of the Reynolds number. This stance was later affirmed by the findings of the Propeller Committee of the ITTC as documented by Allan et al. (1951). Despite these early and insightful contributions, more than seven decades later, the complexities associated with differences in the propeller boundary layer regime between models and full-scale ships remain unresolved.

### 1.2 The Propeller Boundary Layer Challenge

The presence of a laminar or transitional propeller boundary layer poses significant challenges. Primarily, it fails to represent the full-scale turbulent flow, which is what the model tests aim to simulate in order to predict propeller performance. A turbulent boundary layer drastically changes the propeller performance characteristics in terms of drag and lift. This impact on lift is typically ignored when extrapolating model-scale results to full-scale applications using the ITTC 1978 procedure (Aucher et al. 1978). Similarly, laminar boundary layers occurring on model-scale are prone to separation under adverse pressure gradients, leading to flow separation near the propeller trailing edge, which is another factor neglected in this Reynolds scaling procedure. These inconsistencies suggest that an optimally performing propeller at model-scale may not deliver similar performance at full-scale. This calls into question the efficacy of current model-testing methods and the associated extrapolation, especially when comparing different propeller designs and the measured differences are marginal.

Besides the challenge of accurately scaling up to full-scale, the presence of a laminar boundary layer on propeller models introduces additional complexities during testing. The position and occurrence of boundary layer transition, along with laminar flow separation near the trailing edge, heavily depend on the rotation rate of the propeller. This rate varies significantly across different model ship speeds, resulting in unclear trends in propulsion factors, such as the relative rotative efficiency, as explored and elucidated by Li (2019). Furthermore, test conditions like the level of inflow turbulence and water temperature in the experimental facility, both subject to seasonal variations, are also factors that influence these phenomena.

Despite extensive attention and numerous scientific studies, the issue of model propeller scaling remains unresolved due to its intricate and multifaceted nature. First and foremost, amending model test procedures is daunting. Institutes specializing in model testing have built up decades of expertise in executing, evaluating, and extrapolating results using propellers devoid of turbulence stimulation. Generally, this approach yields reliable trial predictions, though unexpected outcomes can still arise. A radical change in testing procedures would necessitate a complete overhaul of their accumulated knowledge and tools. Second, even with advancements in technology, capturing visual data of the model propeller's boundary layer during tests remains challenging. While there are publications showcasing results from visualisation paint tests, the specifics of these methodologies remain undisclosed, as does the intrusiveness level of the paint used. Third, previous attempts to use turbulence stimulation, including methods like leading-edge sand roughness or studs, faced challenges in distinguishing the parasitic drag effect of these elements from changes in the propeller's boundary layer. Finally, given the profound impact of propeller design nuances, pinpointing a consistent trend has been challenging. Certain designs showed more pronounced or even divergent effects compared to others. To understand the observed results, Computational Fluid Dynamics (CFD) simulations can be used, but the obtained results showed to have a strong dependence to the inlet turbulence quantities when using transition modelling, as described by Baltazar et al. (2023). This underscores the need for high-quality experimental data on boundary layer visualisation to support and validate CFD models, which is a key motivation for the current study.

Using turbulence stimulation on model propellers demands not only changes in the experimental approach, but also a revision of the current extrapolation methods. The existing empirical relationships, as outlined for example by the ITTC-78 (Aucher et al. 1978), fall short when enforcing a turbulent propeller boundary layer during model tests. The reason is, that this procedure only corrects for the skin friction and the positive effect on lift generation due to a higher Reynolds number is implicitly accounted for by the fact that the boundary layer is laminar or partially laminar on model-scale.

Both the experimental methodology as well as the scaling procedure requires attention, and in these areas, the International Towing Tank Committee (ITTC) plays a key role by reviewing and providing recommendations. Interestingly enough, the Powering Performance Committee of the ITTC, as early as 1987, recognized the benefits of propeller turbulence stimulation in model tests when combined with an extrapolation procedure that accounts for the Reynolds number effect on lift, for improving the accuracy of powering predictions (Tanibayashi et al. 1987). However, the same committee also identified a significant hurdle: convincing stakeholders, including propeller designers, shipowners and shipbuilders, that a deliberate reduction in efficiency at the model scale induced by turbulence stimulation could actually provide more accurate predictions for the efficiency and power-to-rotation rate ratio of the full-scale propeller.

Concluding, to effect updates in all these areas, well-founded research and consensus among the experts of all fields of expertise are crucial prerequisites. This is not merely a technical challenge, but also one of persuading the industry to embrace a methodology that appears counter-intuitive but promises better full-scale performance predictions.

### 1.3 Evolution of Propeller Boundary Layer Research

One of the earliest publications using paint to visualise a propeller boundary layer dates back to 1940 and was made by Gutsche (1940). He used a paint made from linseed oil,

Turkish red oil and pine soot, which was applied in the form of dots. The paint was used to visualise flow separation, not to determine the boundary layer regime. He applied the paint method to a stationary wing, a rotating wing and concluded with model propellers.

One of the first comprehensive studies into the propeller boundary layer regime was carried out by Meyne (1972). Meyne used several techniques, including paint tests and an electrolytic method, which gave similar results to the paint method, but was technically and practically more demanding and even used hot film probes. The paint used was a commercial paint named Glasurit, type 179-LHO 123.

Another study, conducted by Tamura and Sasajima (1977), is notable for several reasons. Firstly, they published a paint formulation that could be tailored to the Reynolds number. They achieved this by changing the ratio of engine oil and grease to influence viscosity of the paint. They added the pigment titanium white, which consists mainly of titanium dioxide, to colour the oil mixture. The second reason is that they also conducted paint tests for propulsion tests, where it was concluded that the open-water tests and the behind model ship results were very similar. The third is that this was also one of the first applications of turbulence stimulators for model propellers. Their conclusion was that in order to obtain more consistent propulsion factors, an identical boundary layer should be achieved between the open water and propulsion tests. This was achieved using turbulence stimulators, although they observed a large difference in propeller performance due to their use, which they concluded was due to the drag of the stimulators and required further research. Finally, Tamura and Sasjima were also the first to introduce the idea of using two open-water tests. One to determine the propulsion factors and the other to extrapolate the propeller performance to full scale. The aim of this method was to obtain more consistent propulsion factors. This is also the procedure recommended by the ITTC (2002) who called it the 2POT (Propeller Open-water Test) method.

The first application at MARIN of a paint test to visualise the propeller boundary layer was by Kuiper (1978).He employed these paint tests, utilising a commercially available lead-white paint, to study the impact of transition on scale effects in cavitation inception. Kuiper's research led to the pivotal introduction of propeller leading edge roughness in cavitation tests at MARIN. Additionally, he was the first who introduced the idea of adding an fluorescent pigment to the paint and photograph the resulting flow pattern with ultra-violet illumination. This technique of using fluorescent pigments is also adopted in the paint test results presented in this paper.

Boorsma (2000) conducted a study at MARIN to also investigate the potential benefits of leading edge roughness in enhancing the accuracy of full-scale ship powering performance predictions. In his experiments, carborundum was affixed to the propeller's leading edge as a means of turbulence stimulation. This technique, however, was found to be effective only for tripping the boundary flow at the outer radii of the propeller. The effectiveness of this approach was assessed using the paint test method originally introduced by G. Kuiper, albeit with a modification where the traditional lead-white paint was replaced with zinc-white. Despite the innovative approach, Boorsma's study encountered some challenges. Some results were ambiguous, and the discerned trends exhibited inconsistencies. Crucially, Boorsma concluded that an alternative for the ITTC-78 (Aucher et al. 1978) extrapolation procedure would be necessary, for which Boorsma proposed the use of a two-dimensional strip theory. His findings suggested that applying turbulence stimulation to model propellers has the potential to enhance the reliability of full-scale performance predictions. However, the limited number of test cases, coupled with the inconsistent trends observed and the uncertainties surrounding the isolated effects of turbulence stimulation, were not sufficient to necessitate a change in the established experimental procedures.

The challenge to distinguish the effect of the turbulence stimulators from the parasitic drag appeared to be unsolvable and for a while few studies were published with propeller boundary layers as subject. However, the past decade has seen a resurgence of interest in this field for two key reasons. First off, the drive for lower fuel consumption, achieved by reducing ship design speeds and increasing propeller efficiencies, has led to a trend of progressively smaller blade areas and especially these type of propellers seem to cause problems during model tests. This trend was facilitated by advancements in propeller design methods, which brings us to the second reason. As viscous flow simulations evolved into an industry standard for propeller design, the discrepancies between towing tank results and simulations grew too significant to overlook. Consequently, issues of low-Reynolds number performance in propellers, which had been overlooked for an extended period, have once again become pressing.

Streckwall et al. (2013) decided to address the difference in propeller boundary layer regime between model and full-scale using a correction process called 'The Strip Method'. The model tests are still performed without any form of turbulence stimulation, but a correction is applied per radial section, called a strip, on the sectional drag by integrating the laminar and turbulent contributions of the skin friction. This method is now the standard procedure to scale model test propeller performance towards full-scale at HSVA.

In 2015, Bhattacharyya et al. published a numerical study to investigate if using a transition model enhances the comparison with model-test results. This study focused on both a ducted and an open propeller, with the latter also including results from paint tests. Their findings revealed that the transition model provided a better match with experimental data, but the differences were not substantial. They concluded that additional research was needed. Concurrently, at MARIN a similar numerical study was conducted by Rijpkema et al. (2015). Their study highlighted the limitations of fully turbulent CFD simulations in accurately predicting performance, underscoring

the need for transition models. This finding was further supported by Baltazar et al. (2017) in the MARIN-IST collaboration, where the inclusion of transition modelling was shown to significantly reduce discrepancies between experimental data and CFD simulations.

In 2017, Lücke and Streckwall conducted a study with the focus on small area propellers. By means of propeller paint tests using an oil-base paint, it was observed that the propeller boundary layers were largely laminar for both POTs as well as propulsion tests. Additionally, the study explored the trend of obtaining low relative rotative efficiency factors. This exploration involved a comparison between HSVA's Strip Method, the 2POT approach, and a high Reynolds number propulsion test conducted using the HYKAT water tunnel facility. It was found that propulsion tests at low Reynolds numbers consistently resulted in lower relative rotative efficiencies compared to higher Reynolds numbers, with the 'Strip Method' yielding efficiencies on average 1.5% lower than those obtained via the 2POT approach. The study concluded that there was an unaccounted Reynolds scale effect warranting further research. Moreover, Lücke and Streckwall applied turbulence stimulation at the leading edge using a special paint designed to create a rough, rust-like effect. However, this method of turbulence stimulation appeared to have minimal impact. The flow patterns on the painted blades were very similar to those on clean blades, indicating that the applied turbulence stimulation was insufficient to induce boundary layer transition.

Lücke (2019) extended his investigation to explore the diverse trends in relative rotative efficiency across a range of propeller types, including unconventional tip-fin and ice-class propellers. He deduced that the interplay between low-Reynolds scale effects and the propeller's geometric features, such as pitch distribution and thickness-to-chord ratios, markedly influences the trends in relative rotative efficiencies. He substantiated his conclusions using both propeller paint tests, conducted with a black oil-based paint, and a CFD study. The CFD study involved a comparative analysis of fully turbulent and fully laminar flows, excluding transition modelling.

Hasuike et al. (2017) performed an extensive study propeller boundary layers using both experimental paint tests and numerical results with the focus on small blade area propellers. In this study, great care was taken to perform accurate CFD simulations including transition modelling. It was concluded that for both open water tests as well as propulsion tests, the boundary layer was mainly laminar, resulting in large laminar flow separation regions. They emphasized on utilizing numerical tools to obtain more consistent propulsion factors and to improve the scaling procedure towards full-scale.

Li et al. (2019) investigated transitional flows on model propellers, focusing particularly on their impact on relative rotative efficiency. This study involved both paint tests and viscous flow simulations, which included boundary layer transition modelling for three different propellers. The paint tests utilized black toner ink. Li concluded that two primary factors contribute to notably low relative rotative efficiencies when applying the ITTC 1978 powering performance procedure. The first is a moderate discrepancy in Reynolds numbers between the POT and the propulsion test, as defined by the ITTC-78 standard. The second factor is laminar flow separation on the suction side of the propeller blade near the trailing edge, a phenomenon significantly influenced by the Reynolds number. It was also determined that the 2POT method could mitigate discrepancies in relative rotative efficiency, although it has several drawbacks. The study emphasized the need for ITTC members to develop more effective scaling methods for non-conventional propellers.

A common theme in recent studies is that uncontrolled boundary layers in model propellers pose significant challenges. These are mainly seen as unpredictable trends in propulsive efficiency factors, discrepancies with CFD simulations and increased uncertainty in extrapolating results to full-scale conditions. Turbulence stimulation for model propellers can be an effective solution to these problems. However, the general consensus seems to be that the introduction of turbulence stimulation for propellers in model scale experiments is too challenging, as recent publications predominantly advocate to numerically correct for these low Reynolds number effects.

### 1.4 Objective and Approach

This paper diverges from recent research trends by addressing the uncertainties associated with low-Reynolds effects through the application of turbulence stimulation on model propellers, employing a dual-strategy approach. The first part of this approach involves a detailed study on conducting high quality boundary layer visualisation paint tests. These types of tests are instrumental in elucidating the effects of turbulence stimulation on model propellers and also serve as a validation data for CFD simulations. The second aspect is a novel method for inducing turbulence efficiently, characterized by the simplicity of the 'turbulators' design and their ease of application to a model propeller. Moreover, the paper investigates and delineates how the turbulators drag affects the propeller performance. It should be noted that the critical aspect of Reynolds scaling from model to full-scale via CFD is not addressed in this paper, but is extensively covered in Kerkvliet et al. (2024).

## 2 METHODOLOGIES

### 2.1 Test-Case Propellers

To demonstrate the different trends that can occur when applying turbulence stimulation, four modern design propellers are presented in this paper. The main particulars of the propellers are given in Table 1. All four propellers are part of MARIN's stock propeller portfolio and represent diverse types with variations in expanded blade area ratio and pitch.

**Table 1: Characteristics of the four test-case propellers**

| | | | |
|---|---|---|---|
| Propeller-A | Diameter | $D$ | 289.6 mm |
| | Number of blades | $Z$ | 5 |
| | Chord at 0.7R | $c_{0.7R}/D$ | 0.2706 |
| | Pitch | $P_{0.7R}$/D | 0.87 |
| | Expanded Area Ratio | $A_e/A_o$ | 0.613 |
| Propeller-B | Diameter | $D$ | 300 mm |
| | Number of blades | $Z$ | 5 |
| | Chord at 0.7R | $c_{0.7R}/D$ | 0.2789 |
| | Pitch | $P_{0.7R}$/D | 1.045 |
| | Expanded Area Ratio | $A_e/A_o$ | 0.6362 |
| Propeller-C | Diameter | $D$ | 290 mm |
| | Number of blades | $Z$ | 4 |
| | Chord at 0.7R | $c_{0.7R}/D$ | 0.1766 |
| | Pitch | $P_{0.7R}$/D | 1.60 |
| | Expanded Area Ratio | $A_e/A_o$ | 0.35 |
| Propeller-D | Diameter | $D$ | 290 mm |
| | Number of blades | $Z$ | 4 |
| | Chord at 0.7R | $c_{0.7R}/D$ | 0.4783 |
| | Pitch | $P_{0.7R}$/D | 1.00 |
| | Expanded Area Ratio | $A_e/A_o$ | 0.85 |

### 2.2 Flow Visualisation Paint

To visualise a propeller boundary layer during a towing tank experiment is a considerable challenge. Where during wind and water tunnel experiments there are possibilities to use Laser Doppler Velocimetry or possibly Particle Image Velocimetry, this becomes exceptionally difficult in a towing tank setup. Basically the only practical technique available is using a paint to visualise the boundary layer flow.

When used appropriately on a propeller, paint, which is commonly employed to visualize flow direction and identify flow separation, can also effectively reveal the characteristics of the boundary layer. When the boundary layer becomes turbulent, the local frictional stress exerted on the blade by the fluid increases drastically. Since the exerted centrifugal force remains constant, this increase in frictional stress leads to a change in both magnitude and direction of the local friction force on the blade surface when transition occurs. This change is visibly indicated by the streaks of paint on the blade surface (Kuiper 1981).

To facilitate the understanding and interpretation of propeller paint test results, we present an illustrative example accompanied by a graphical depiction in Figure 1. In the area where the boundary layer remains laminar, the streaks take on a somewhat tangential direction and exhibit a purple hue. At the juncture where transition takes place, there is a distinct shift in both the direction of the paint streaks, which become more radial, and in the colour of the paint. This change in colour is due to the higher friction force, leading to a thinner layer of paint compared to the area of laminar flow. At the lower propeller radii near the trailing edge, a laminar separation region is evident. Here, the streaks are also radial in direction, yet they differ markedly from those in the turbulent region. Moreover, at the separation line, there is a noticeable accumulation of paint, a feature absent where transition occurs.

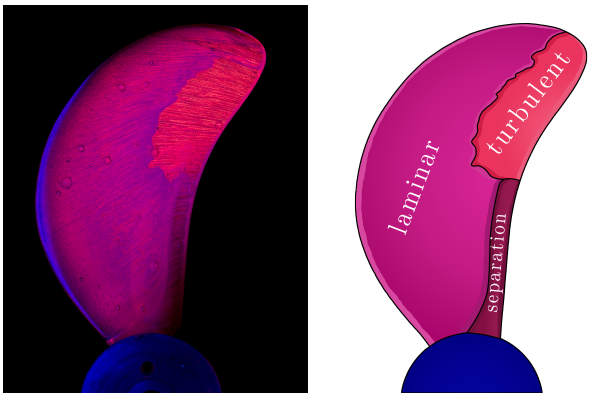


**Figure 1: A paint test result (left) with a schematic representation (right) detailing different types of boundary layer flow.**

To develop a flow-visualisation paint suitable for everyday application in projects and consultancy tasks, the following four requirements were established:

- The paint must yield clear and unambiguous results, minimizing the need for subjective interpretation.
- The paint should minimally impact the boundary layer flow to ensure the accuracy of the paint test results.
- The composition of the paint must be suitable for a wide range of model-scale propeller operational conditions.
- The paint should be either easy to acquire or to produce.

For the boundary layer visualisation paint, three key properties are critical. The first is the yield stress, which determines the minimum amount of stress needed for the paint to start flowing. A low yield stress is essential to ensure that the paint begins to flow even under conditions with relatively low frictional forces, such as those found on the lower radii of a propeller. The second important property is viscosity, a measure of the resistance to deformation at a given rate in a fluid. Once the yield stress is overcome, it is the viscosity that primarily governs the flow of the paint. Ideally, the paint should be relatively viscous to ensure that it flows slowly over the blade during the experiment. This characteristic makes the results less sensitive to the start-up phase and the overall duration of the experiment. Additionally, a higher viscosity simplifies the application process, preventing the paint from running off the blade before the experiment commences. However, it is crucial that the paint is not so viscous that it continues to affect the boundary layer flow until the end of the experiment. Finally, the density of the paint should be approximately similar to that of water. This similarity in density helps in maintaining the natural flow characteristics around the propeller, ensuring that the paint's presence does not unduly influence the results.

Modern commercial paints are advanced technological compounds where many more properties than only the viscosity and yield stress are of importance, such as for example drying time, coverage level and ageing properties. As most of these paint characteristics are not relevant for this application and to have complete control over the oil

base and pigment mixtures, it was decided to produce the paint in-house.

Contrary to what one might initially assume, this process is surprisingly straightforward. For our purposes, the paint only needs to consist of two primary components: an oil and a pigment. This simplicity allows for the customization of the paint to meet our exact requirements, focusing on the essential properties needed for effective flow visualisation without the unnecessary complexities of commercial paint formulations.

Adopting the strategy pioneered by Kinya Tamura & Takao Sasajima (1977), our paint formulation utilizes two types of oils, allowing us to tailor the mixing ratio according to the Reynolds number being tested. While Tamura and Sasajima achieved the desired viscosity using a mixture of engine oil and grease, we opted for a more uniform oil base. Our approach employs two oils with a significant difference in viscosity: a high-viscosity stand oil and a low-viscosity linseed oil. Essentially, both are the same substance, with stand oil being linseed oil that has undergone heat treatment to increase its viscosity.

The second fundamental component in our paint formulation is the pigment. In 1981, Kuiper employed a commercial paint containing lead-white pigment, a choice favoured by artist painters since the 17$^{th}$ century due to its low yield stress which facilitates easy flow, an essential characteristic for effective flow-visualisation paint. However, the toxicity of lead-white and its associated health risks necessitated a transition to safer pigments. In 2000, Boorsma substituted lead-white with zinc-white, but this proved to be a suboptimal choice as zinc-white has a considerably higher yield stress than lead-white, thereby adversely affecting the paint's flow properties. The nuances in yield stress and their implications are extensively analysed by Salvant Plisson (2014). A more fitting alternative, as also adopted by Tamura and Sasajima in 1977, is titanium-white. This pigment is non-toxic and provides similar flow characteristics to lead-white, making it an excellent contemporary replacement. Significantly, titanium-white has also emerged as the pigment of choice for modern artists, serving as a safer substitute for lead-white.

The distinctive component that sets the flow-visualisation paint method presented in this paper apart, and differentiates it from other propeller paint visualisation techniques, was introduced by Kuiper in 1981. This key ingredient is a pink daylight fluorescent pigment, manufactured by the DayGlo Color Corp. When combined with titanium white, this fluorescent pigment produces more vivid flow streaks, which are crucial for effective and clear flow visualisation of propeller boundary layer flows.

While this paper does not detail the specific ratios of oils and pigments in the paint formulation, these details can be provided upon request.

### 2.3 Ultra-Violet Photography

Capturing a high-quality paint test photograph is more challenging than it initially appears, necessitating several iterations to perfect the methodology. To provide clarity on this process, a brief description of the photographic setup making use of ultra-violet (UV) illumination is presented. Six key components are essential for taking high-quality photographs in this context: a source of UV light, a camera equipped with a macro objective lens, an UV filter, a remote trigger control, a green cardboard background, and a reliable camera mounting system.

When fluorescent pigments in the paint are exposed to UV light at a wavelength of 265nm, they emit a visible pink-red glow of relatively low intensity. The UV light source used is a custom-made LED panel that can be attached to the camera's objective lens using a clip-on mount originally intended for a solar hood. This LED panel consists of a total of 336 LEDs with a combined power of approximately 50W. A diffusion filter was added to the lamp to prevent individual LEDs from reflecting off the painted propeller surface.

The second key component is the camera. A Nikon D850 full frame camera with a 45.7 megapixel sensor was used. The lens used was the AF-S VR Micro-NIKKOR 105mm, which is renowned for its sharpness. A UV filter was used to capture only the emitted light from the fluorescent particles, preventing any reflected UV light from reaching the camera sensor, as this can cause a blue haze and reduce the contrast. To avoid motion blur, the camera was triggered using a Nikon MC-36A remote control. The camera's ISO setting was set to 100, the aperture was set to f/14 to ensure sufficient depth of field, and the shutter speed was approximately 20 seconds. A green piece of cardboard was used under the propeller to allow the background to be easily removed using a graphics editing software package. Figure 2 shows the complete setup used to take the photographs of boundary layer flow using paint tests as presented in this paper.

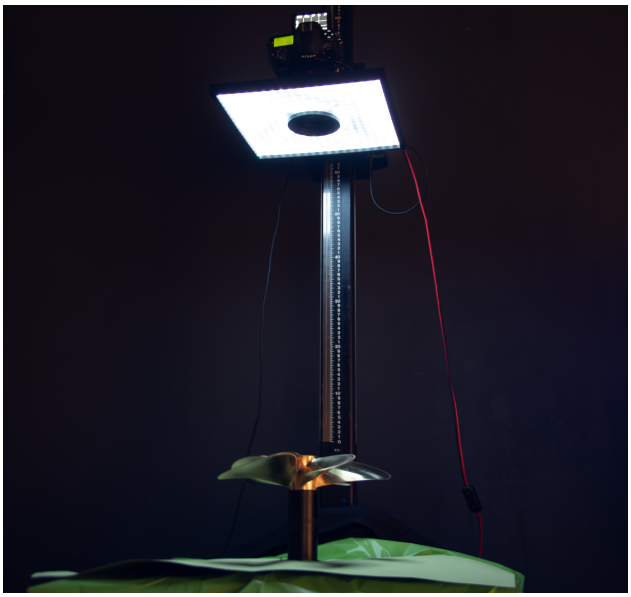

**Figure 2: The UV photography setup for capturing boundary layer flow using paint tests.**

To illustrate the importance of capturing photographs using

a UV light source, we present a comparison with a regular light source in Figure 3. When observing the propeller under regular lighting conditions, the oil paint layer is hardly visible due to its extremely thin and almost transparent nature, causing the metal blade surface to reflect most of the incident light. However, when using UV light, the reflected UV radiation from the metal surface is selectively filtered by means of an UV filter, allowing the camera to capture only the emitted light from fluorescent pigments. This reveals the intricate flow patterns within the boundary layer.

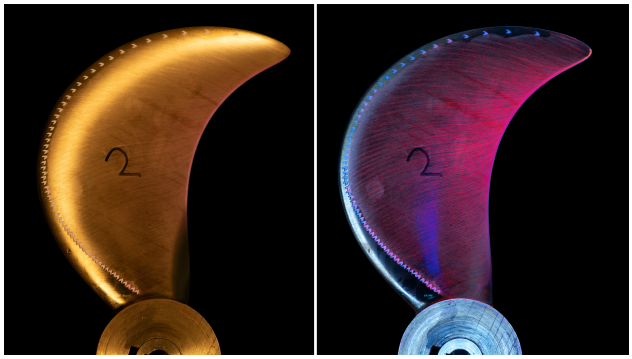

**Figure 3: A comparison between a regular light source (left) and an UV light source (right).**

### 2.4 Experimental Setup and Procedure

The process of performing a propeller paint test is largely similar to a standard open water test but includes a few key modifications. The initial step involves the application of paint to all the propeller blades, with the exception of one left unpainted for handling purposes. Each blade is treated with either a slightly varied paint composition or a different application area to assess the sensitivity of the results. Applying paint specifically on the leading edge is more effective for identifying flow separation, whereas painting the entire blade ensures visualisation of the near wall flow of the complete blade.

Following the paint application, the next step involves mounting the propeller onto the open-water test setup, as shown in Figure 4. This new setup is equipped to measure thrust up to 2000 N, a torque of up to 100 Nm, and a rotation rate of 2500 rpm.

The open-water propeller setup is then submerged, positioning the propeller shaft at a depth of 0.9 metres. The third phase of the test involves conducting the open-water test at a constant advance coefficient J. Maintaining a constant advance coefficient from the beginning is preferred to minimize the start-up procedure's impact on the results. However, a variation in the Reynolds number during the start-up phase is inevitable. The duration of the start-up phase is limited by the maximum allowable acceleration of the carriage, with the goal of keeping this phase as brief as possible by opting for a relatively high maximum acceleration. The limits of acceleration are dictated by the capabilities of the testing facility; in the Deep Water Tank (DT), the maximum acceleration is $0.7m/s^2$, while the Concept Basin (CB), formerly the High-Speed Tank (HT), can accommodate higher accelerations. A comparison within the CB of maximum accelerations of $0.45m/s^2$ and $0.9m/s^2$ demonstrated that the difference in acceleration had a negligible effect on the results.

Finally, upon completion of the test run, the open-water test setup is immediately raised before the carriage returns to the starting point of the towing tank. At this stage, the propeller is carefully removed, now prepared and ready for photographic analysis.

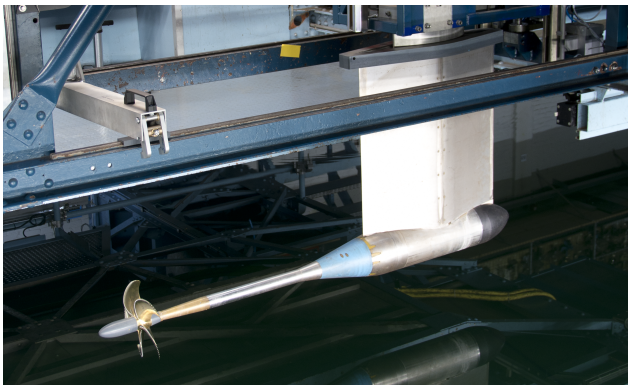

**Figure 4: The experimental open-water propeller test setup.**

### 2.5 Propeller Turbulence Stimulation

Sand roughness stands as one of the earliest methods for tripping a boundary layer in fluid dynamics experiments. Within the specific field of model propeller testing, leading edge sand roughness is commonly employed, primarily aimed at cavitation inception rather than actively inducing turbulence. Thus, the exploration by Boorsma (2000) to utilize leading edge sand roughness as a means to induce a turbulent boundary layer can be seen as a logical initial step. Yet, this technique comes with certain drawbacks, particularly in terms of consistency and practicality. These limitations have led to the exploration of alternative methods for turbulence stimulation. Among these, one method has emerged as particularly promising. This section will delve into both the traditional application of sand roughness and this new and effective method.

#### *2.5.1 Sand Roughness*

As mentioned afore, sand roughness is one of the earliest methods of promoting early boundary layer transition. Already in in 1958, Braslow and Knox (1958) conducted extensive and foundational research on sand roughness as a turbulence stimulation method by means of wind tunnel tests on air foils. They provided a critical insight into the required sizes of the sand grains required to induce transition based on the undisturbed flow velocity at the trip height. Transition will be realised if the critical Reynolds number $Re_h$ is in the range of 250 to 600, with the $Re_h$ defined as:

$$Re_h = \frac{u_h h}{\nu}. \tag{1}$$

In Equation 1, $\nu$ represents the kinematic viscosity, $h$ denotes the height of the roughness element and $u_h$ is the undisturbed flow velocity at the height of the roughness element. Following a practical engineering approach, the

velocity profile of a laminar boundary layer over a flat plate can be approximated as parabolic. This approximation aligns with the method employed by von Kármán, as discussed in White (2010).

$$u(x,y) \approx U_\infty \left( \frac{2y}{\delta} - \frac{y^2}{\delta^2} \right) \qquad 0 \leq y \leq \delta(x) \qquad (2)$$

In Equation 2, $x$ is the measure from the leading edge to the roughness element in stream-wise direction. The $y$ is the distance from the wall, which can be set equal to $h$. Additionally, $\delta$ represents the boundary layer thickness. The $U_\infty$ is the free-stream velocity, which can for a propeller be assumed to be approximately equal to the local propeller velocity $V_{r/R}$.

$$V_{r/R} = \sqrt{V_a^2 + \left( \frac{r}{R}\, \pi\, n\, D \right)^2} \qquad (3)$$

In Equation 3, $V_a$ represents the advance velocity of the propeller, the $n$ denotes the propeller rotation rate, and $D$ refers to the propeller diameter.

The boundary-layer thickness $\delta$ is approximated by $\delta_{99}$. This approximation corresponds to the point at which the flow velocity $u$ reaches 99% of the free stream velocity $U_\infty$. From this definition, an estimation for $\delta_{99}$ can be derived using the Blasius solution for a laminar boundary layer:

$$\delta_{99} \approx 5 \frac{x}{\sqrt{Re_x}}. \qquad (4)$$

In Equation 4, $Re_x$ is the local Reynolds number and is defined as:

$$Re_x = \frac{x V_{r/R}}{\nu} \qquad (5)$$

Utilizing the relevant equations allows an estimation of the necessary sand roughness grit size. As an illustrative example, consider Propeller A (described in Table 1) operating at an advance coefficient J = 0.8 with a rotation rate of 800 rpm. To effectively trip the boundary layer with sand roughness at 0.7R, 2.5 mm from the leading edge, a critical Reynolds number ($Re_h$) of 600 is required, in line with the findings of Braslow and Knox. This criterion leads to the determination that the height of the sand roughness ($h$) should be approximately $73\mu m$ at 0.7R.

As mentioned earlier, there are several drawbacks of using sand roughness as turbulence stimulation. The very first issue of using sand roughness as turbulence stimulation originates from the the way the particles are produced. Although the common terminology for turbulence stimulation with small particles is sand roughness, what is actually used at MARIN is silicon carbide, also known under the name carborundum. During the production process, the silicon carbide is crushed and sieved. The crushing results in sharp edged particles, which is excellent for turbulence stimulation, but they can have a non-cubical shape. As a result, the particles that are selected during the sieving process to be within a certain size range, can actually have a dimension in one direction that is way outside the specified range.

For the carborundum roughness, the different grit sizes were compared. The smallest, henceforth denoted as S, supposes to have a size variation between the range of $53 - 62\mu m$. The mid sized grains, denoted with M, have a size range of $88 - 105\mu m$ according to the specifications. The largest grains, indicated with the letter L, have a range of $177 - 210\mu m$. By using a microscope calibration grid, an insightful comparison could be made to visualise the comparison in specified grain sizes and actual grain size and the variation in size, see Figure 5. The white rectangles are the specified dimensions, where it becomes evident, that there is a large variation in particle sizes and also many grains greatly exceed the specified dimensions. It is important to realise that for most particles, the third dimensions is probably as specified.

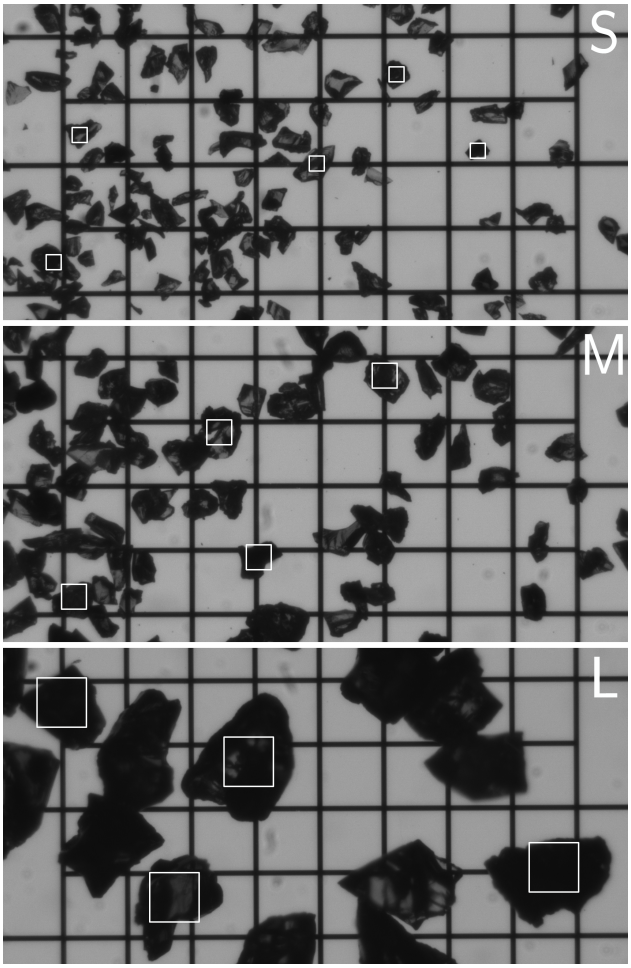


**Figure 5: Microscopic view of three carborundum size variants - Small (S) ranging from 53 to $62\mu m$, Medium (M) from 88 to $105\mu m$, and Large (L) from 177 to $210\mu m$, placed on a microscope calibration grid. The white reference squares indicate the intended target sizes for each particle size category.**

Secondly, applying sand roughness requires precision, as adhesive must be used sparingly to avoid submerging the sand grains in glue, thereby maintaining their effectiveness in inducing transition. This conscientious task demands the skill and experience of the individual applying it. Thirdly, applying sand roughness to both the suction and pressure sides separately is cumbersome and is therefore applied

simultaneously to both sides of the propeller, including the leading edge. This leads to the inadvertent alteration of the propeller's leading edge. Fourthly, ensuring a uniform distribution of sand grains is challenging. Overly dense placements cause the grains to be act as a single bump in the flow, instead of individual particles creating separate vortex pairs. Moreover, given that the Reynolds number varies along the propeller radius, the grit size should accordingly change in size along the propeller radius. This variation, however, proves to be challenging and, at best, is impractical. Another point of attention is, especially for the lower radii, straight on the leading edge itself is not the most efficient position to trip the flow. Moreover, the sand roughness strip is prone to damage through contact or degradation over time due to environmental exposure, and such damage is often not readily apparent to the naked eye. Lastly, applying sand roughness is a time-consuming task that necessitates patience and should not be hurried.

#### *2.5.2 Turbulators*

In light of the drawbacks associated with using sand roughness, as discussed in the previous section, this study introduces a novel technique for inducing a turbulent boundary layer on model propellers. This method, inspired by the zigzag strip concept (Lyon et al. (1997) and Elsinga & Westerweel (2012)), is characterized by minimal additional drag and enhanced repeatability in testing. A zigzag strip efficiently trips the boundary layer, generating vortices that evolve into arch-shaped structures and further develop into the hairpin structures typical of a wall-bounded fully turbulent boundary layer.

However, direct application of a continuous zigzag strip along the leading edge of a propeller, especially one with significant skew, will result in severe misalignment with the flow at the higher radii. Such misalignment diminishes the strip's effectiveness in tripping the flow. To address this issue, the continuous strip is modified into separate, smaller elements. These elements are strategically distributed along the leading edge and individually aligned in the tangential direction. This modification ensures effective flow tripping even for highly skewed propellers.

These individual elements are very similar to the idea patented by Wheeler (1991). Such a turbulator can generate a twin-vortex that promotes a turbulent boundary layer at the cost of minimal drag. The reason is that this vortex pair closely resembles the hairpin-like vortical structures crucial to the boundary layer transition process. This resemblance facilitates the formation of a turbulent boundary layer with least effort.

The turbulators are tailored to the propeller design and require a number of steps to be made and applied. The first step in the fabrication process involves using a CAD (Computer-Aided Design) package to automatically generate the correct pattern of aligned turbulators along the leading edge, designed for the target propeller. Following this, the turbulator array is fabricated using a cutting plotter, which carves the shapes out of vinyl foil. Subsequently, the excess foil material is removed, leaving only the turbulators, now shaped to match the propeller's leading edge, adhered to the backing foil. A transparent transfer foil is then applied over the turbulators. This transfer foil aids in the removal of the turbulators from the backing foil and enables the simultaneous application of all the turbulators onto either the suction or pressure side of the propeller in a single handling step.

This method effectively addresses the limitations associated with sand roughness. First, the geometry of the turbulators is accurately defined using CAD, along with reference markers such as the propeller tip and leading edge shape. This ensures precise and easy application. Second, this approach maintains the integrity of the leading edge geometry, unlike the sand roughness method. Third, when allowed sufficient drying time, the turbulators are securely attached due to the high-tack adhesive used. Additionally, any damage to or removal of a turbulator is immediately noticeable, allowing for prompt repair. A comparison between sand roughness and the turbulators is illustrated in Figure 6.

Rooij and Timmer (2003) have pointed out that a zigzag is significantly more effective in tripping the boundary layer than sand roughness. They claim that a zigzag strip requires a critical Reynolds number $Re_h$ of just 200, as defined in Equation 1. However, it is important to note that in that specific publication, their claim is not substantiated with scientific proof. In the same context as the example provided in Section 2.5.1, where the required height of sand roughness was determined to be $73\mu m$, applying the same conditions leads to a calculated turbulator height of approximately $36\mu m$. For illustrative purposes, it's noteworthy that the cylindrical and square studs used by Tamura and Sasajima (1977) as turbulence stimulators ranged in size from $265\mu m$ to as high as $900\mu m$.

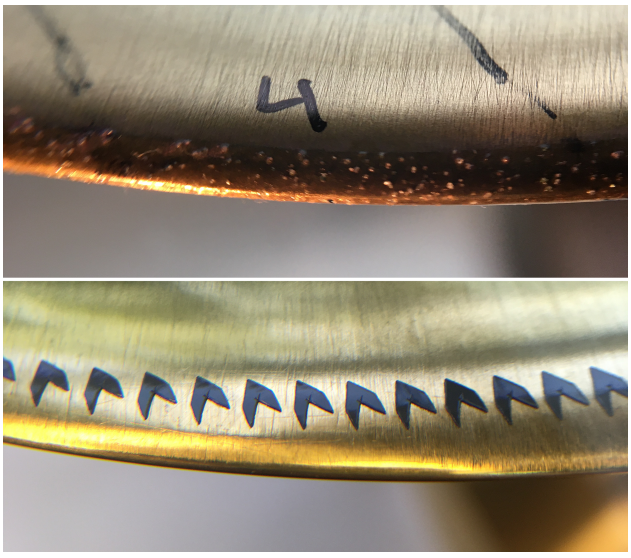

**Figure 6: Two types of turbulence tripping techniques: sand roughness (top) and turbulators (bottom).**

## 3 RESULTS

This section discusses three distinct aspects. The first is the methodology for obtaining the paint composition and the

key points of consideration. The second aspect involves an attempt to estimate the sole effect of the turbulence stimulation method on propeller performance. Finally, we compare the change in propeller performance between laminar and turbulent boundary layers for three different propellers. Central to these discussions is the propeller Reynolds number, for which we use the standard ITTC definition, given by:

$$Re = \frac{c_{0.7R}\sqrt{V_a^2 + (n\pi 0.7D)^2}}{\nu}, \tag{6}$$

where the $c_{0.7R}$ denotes the propeller chord length at 0.7R.

For completeness, the dimensionless key parameters for propeller performance characteristics, specifically the advance coefficient $J$, the thrust coefficient $K_T$, the torque coefficient $K_Q$, and the open water efficiency $\eta_O$, are also provided:

$$J = \frac{V_a}{nD} \tag{7}$$

$$K_T = \frac{T}{\rho n^2 D^4} \tag{8}$$

$$K_Q = \frac{Q}{\rho n^2 D^5} \tag{9}$$

$$\eta_O = \frac{JK_T}{2\pi K_Q} \tag{10}$$

In Equation 8 the symbol $T$ denotes the thrust and $\rho$ represents the water density, while in Equation 9, the symbol $Q$ stands for the propeller torque.

### 3.1 The Flow-Visualisation Paint

This results section discusses the effect of the difference in volumetric pigment content and oil base viscosity is discussed. As introduced in Section 2.2, two properties of the paint are important, the viscosity and the yield stress. The yield stress of the paint, which is not measured directly, is mainly influenced by the volumetric pigment content, while the paint viscosity is a result of both the oil base viscosity as well as the volumetric pigment content.

Starting with the volumetric pigment content, increasing the pigment content will increase both the yield stress and the viscosity. Therefore, the pigment content should be relatively low, yet still be sufficient to visualise the boundary layer flow. The effect of a variation in pigment content can be seen in Figure 7. Excessively high pigment content makes the paint too viscous, leading to high yield stress and potentially causing premature boundary flow transition. Since the transition point remains consistent at lower pigment contents, we are confident that the paint does not influence this transition. Notably, streaks are only visible with the two lowest pigment contents. These streaks, resulting from the presence and absence of paint particles, require a very thin paint layer for visibility. A thicker layer, due to high viscosity, constantly covers the blade with pigments, obscuring streak visibility. To demonstrate that streak visibility is affected not only by pigment content but also by oil viscosity, we compared two samples with equal pigment content but differing oil viscosities, as shown in Figure 8.

To further demonstrate the influence of the base oil viscosity, a variation is presented in Figure 9. If the paint is excessively viscous, the layer remains too thick, preventing streak formation and hindering the paint's ability to flow over the blade. Conversely, if the paint is not viscous enough, the acceleration phase overly influences the results, or the paint washes off the blade entirely. Achieving the desired result involves adjusting the ratio between stand and linseed oil, as detailed in Section 2.2.

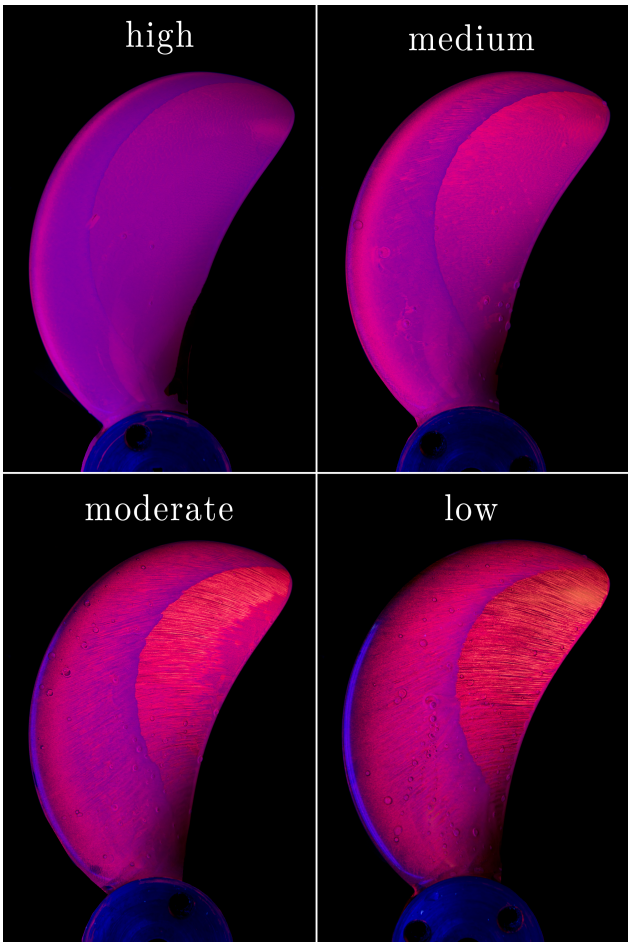


**Figure 7: Impact of varying the volumetric pigment content from high to medium, to moderate, and to low, while maintaining a constant oil base viscosity for the Propeller-A operating at $J = 0.65$ with 900 rpm ($Re = 7.2 \times 10^5$).**

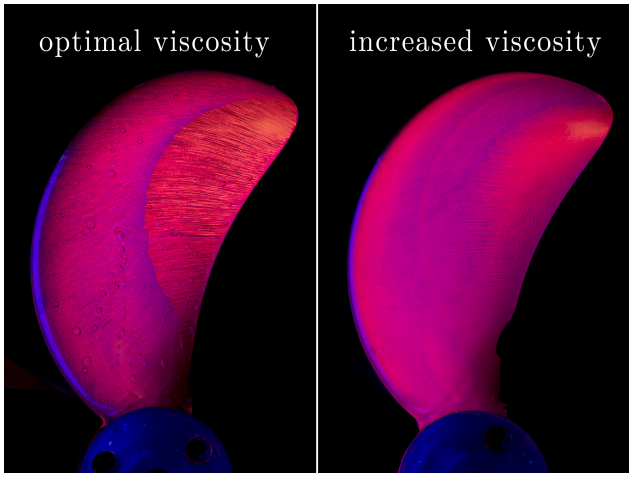


**Figure 8: Comparison of equal pigment volumetric pigment content, but a difference in oil base viscosity for Propeller-A operating at $J = 0.65$ with 900 rpm ($Re = 7.2 \times 10^5$).**

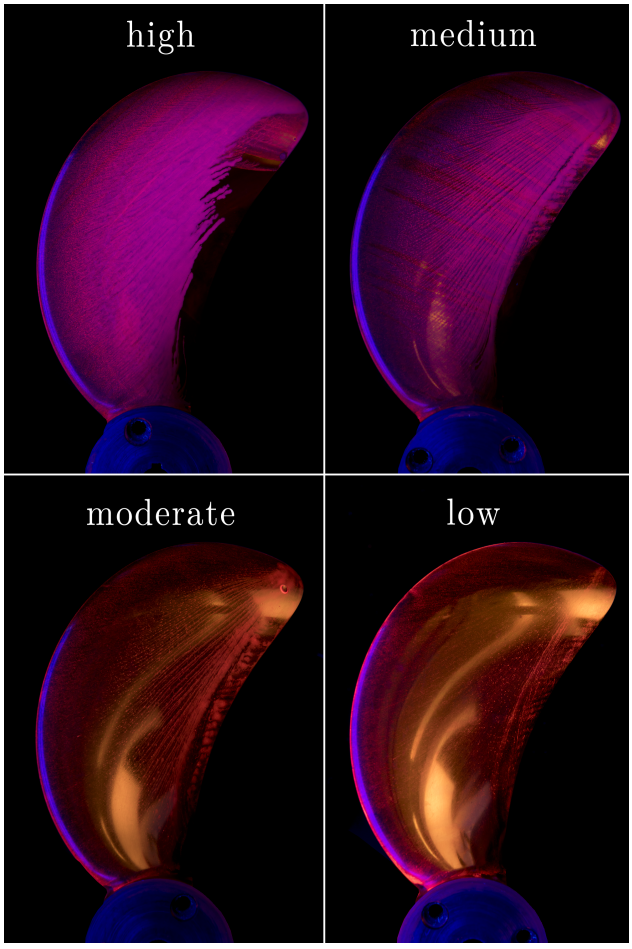


**Figure 9: Impact of varying oil base viscosity while maintaining constant volumetric pigment content for Propeller-A operating at at $J = 0.65$ with 400 rpm ($Re = 3.2 \times 10^5$).**

### 3.2 Effect of Flow Visualisation Paint on the Boundary Layer Flow

One of the important requirements as stated in Section 2.2, is that the flow-visualisation paint does not alter the boundary layer flow. This was investigated in two different ways. The first method was the sensitivity of the transition location for small changes in paint composition. The second method was a more quantitative method, namely by observing the propeller characteristics convergence during an open water experiment and comparing the results with the propeller without flow visualisation paint.

A comparison of the experimentally measured thrust of a propeller without propeller paint, denoted as reference, is compared to a propeller paint test in Figure 10. After the acceleration phase, approximately 7 seconds, the paint is still influencing the flow around the propeller blades until approximately 28 seconds. At this point the thrust is more or less equal to the blade without paint.

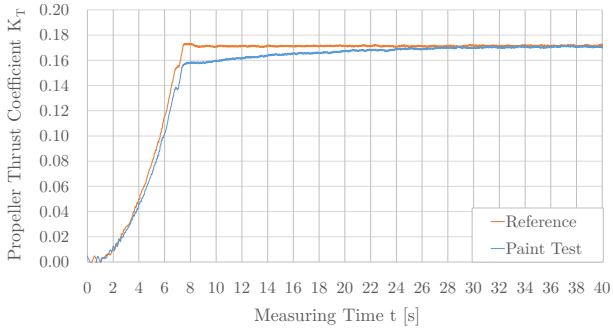


**Figure 10: Thrust convergence history of an open water experiment for Propeller-B without flow-visualisation paint (Reference) and with flow visualisation paint.**

### 3.3 Boundary Layer Flow Visualisation of Propeller-B for a Reynolds variation

The paint test results presented in this section, see Figure 11, pertain to Propeller-B, which was tested under three distinct Reynolds numbers, as detailed in Table 2. The discussion of these results is twofold in purpose. Firstly, they demonstrate that the new paint formulation is applicable across a wide range of Reynolds numbers. They highlight that, in practice, conducting tests at higher propeller Reynolds numbers makes it easier to obtain high-quality paint test results. Secondly, the results show that a partially laminar boundary layer can be maintained even at relatively high Reynolds numbers.

In the ITTC-78 Performance Prediction Methods (ITTC 2017) a minimum $Re_{c_{0.7R}}$ of $2 \times 10^5$ recommended. Although the lowest Reynolds Number exceeds this minimum, it does exhibit a largely laminar boundary layer with massive flow separation on both suction and pressure side. Only at the higher radii on the pressure side is a transition to a turbulent boundary layer visible, as evidenced by the layer becoming thinner and the streaks changing direction. By increasing the $Re_{c_{0.7R}}$ to $9.33 \times 10^5$, the flow separation is no longer present at the pressure side as the transition occurs. Also at the suction side a transitional flow can be observed near the trailing edge at the radii above $\sim 0.7R$. However, the largest part is still laminar with trailing edge flow separation for the lower radii. By increasing the $Re_{c_{0.7R}}$ even further, the transition occurs at all radii for both propeller sides, although still practically half of the total blade surface covered by a laminar boundary layer. We emphasize, for this condition, the

Reynolds number is an order higher than the recommended Reynolds number by the ITTC-78 extrapolation procedure.

**Table 2: The operational conditions of Propeller-B as used in the Reynolds variation study**

| condition # | I | II | III |
|---|---|---|---|
| Re [-] | $3.73 \times 10^5$ | $9.33 \times 10^5$ | $1.49 \times 10^6$ |
| J [-] | 0.8 | 0.8 | 0.8 |
| $V_a$ [m/s] | 1.6 | 4.0 | 6.4 |
| n [rpm] | 400 | 1000 | 1600 |

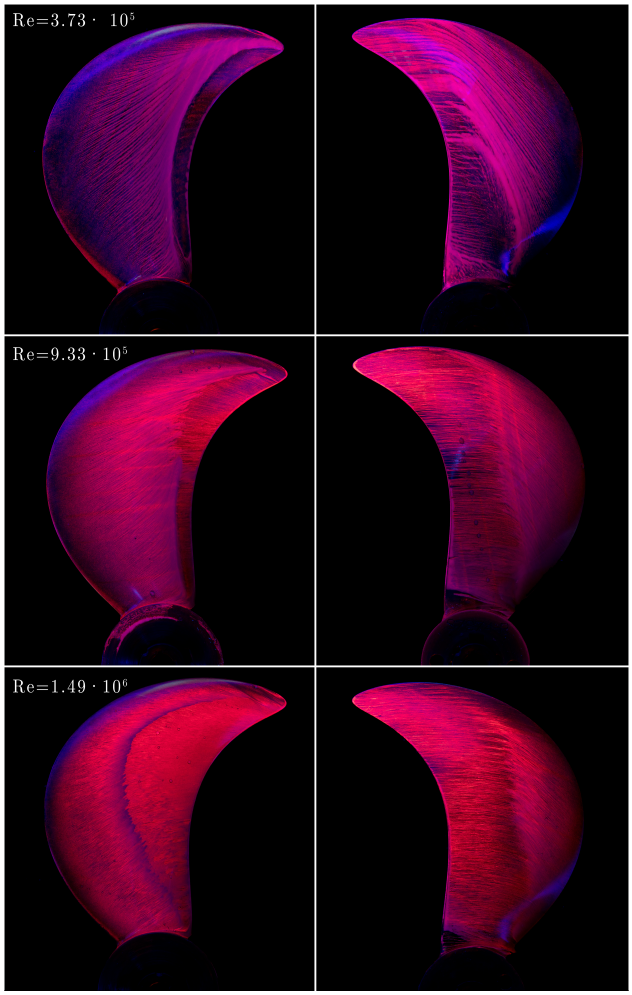


**Figure 11: The change in boundary layer flow of Propeller-B as a function of Reynolds number for the suction (left) and pressure (right) side at design condition $J = 0.8$.**

### 3.4 The Isolated Impact of Turbulence Stimulation on Propeller Performance

As highlighted in Section 1.2, a major challenge in adopting turbulence stimulation as an model-testing standard lies in distinguishing the effects of boundary layer transition from the performance reduction caused by the drag associated with turbulence stimulation. To clarify, inducing a boundary layer transition requires per definition a momentum loss, manifested as drag from the turbulators. However, the turbulence stimulation should not give a significant larger penalty on the propeller performance than necessary to realise transition. To accurately evaluate the isolated impact of turbulence stimulation, we conducted two separate experimental campaigns using Propeller-B. The first focused on sand roughness, while the second investigated the use of novel turbulators. In both experiments, our objective was to vary the height of the turbulence stimulation while ensuring that even the smallest height was sufficient to induce a boundary layer transition. This was crucial to ensure that we were measuring the effects of height variation rather than changes in the boundary layer regime.

Our methodology began by initially applying turbulence stimulation with the smallest height. Subsequently, we utilised flow-visualisation paint to pinpoint the smallest radius at which the transition occurred immediately after the turbulence stimulation. We then removed the turbulence stimulation elements for the radii below this transition point. This identified minimal radius was consistently used as the starting point for experiments with higher turbulence stimulation elements, maintaining the integrity of our assessment of turbulence stimulation's isolated impact.

In the experiments concerning sand roughness, as detailed in Section 2.5.1, various grit sizes were evaluated. For the sand roughness size S, flow-visualisation paint was used to determine that the critical radius was equal to 0.6R. Based on this finding, turbulence stimulation was removed for radii lower than 0.6 r/R. Also the larger sand roughness types M and L were applied starting from 0.6R to the propeller tip. Consequently, for these tests, the propeller boundary layer remained laminar up to approximately 0.6R and transitioned to turbulent at higher radii. The results of these tests are presented in Figure 12.

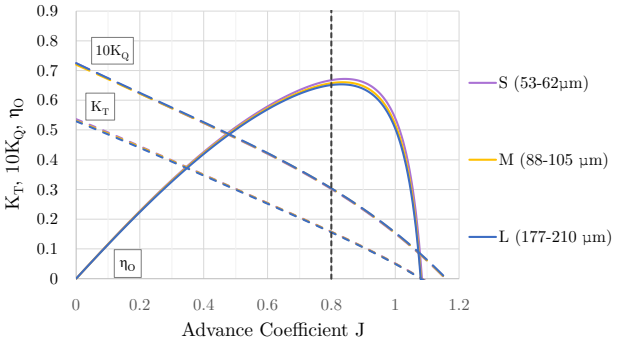


**Figure 12: Open water diagram of Propeller-B performed with a rotation rate of 800 rpm for various leading edge sand roughness heights.**

The comparative analysis of the three sand roughness heights is depicted in Figure 13. The data are presented as relative percentages, with each value normalized to the smallest roughness height for clarity. The most significant effect of over-tripping is observed on the thrust coefficient. When the grain size is increased from S to M, there is a 0.9% increase in the thrust penalty. Further increasing the grain size results in a thrust penalty increase to 1.7%. In contrast, the impact on the torque coefficient appears to be smaller.

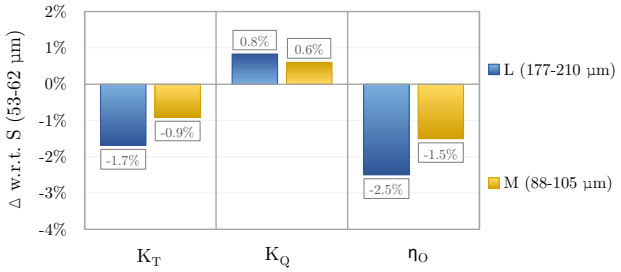


**Figure 13: Influence of the sand roughness height on the propeller performance at design condition $J = 0.8$ with 800 rpm ($Re = 7.5 \times 10^5$).**

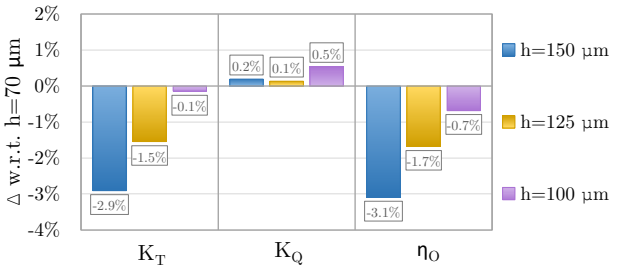


**Figure 15: Influence of the turbulator height on the propeller performance at design condition $J = 0.8$ at a rotation rate of 800 rpm ($Re = 7.5 \times 10^5$).**

A similar study was conducted to assess the drag penalty associated with turbulators. In this exercise, four different turbulators, made from vinyl foils and ranging in turbulator thickness $h$ from $70\mu m$ to $150\mu m$, were tested. To provide a sense of scale, the thinnest turbulators, when scaled up to full-scale propeller dimensions, would have an approximate height of only 2.0 mm.

The effectiveness of the turbulators was such that even the minimal turbulator height was sufficient to trip the boundary layer across the entire blade, a finding confirmed through paint tests. Consequently, increasing the turbulator height beyond this point led to 'over-tripping,' resulting in a non-necessary penalty on the propeller performance.

The open water performance results for these varying turbulator heights are presented in Figure 14. Notably, even though the turbulator height more than doubled, the impact on performance was relatively small. The relative performance differences, when compared to the smallest turbulator height, are illustrated in Figure 15. Mirroring the findings from the sand roughness grit size variation, the most significant effect was observed on thrust, while the variations in torque were minimal.

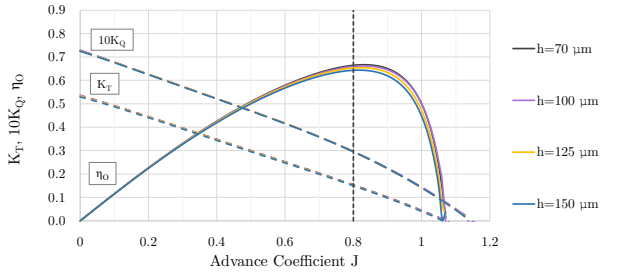


**Figure 14: Open water diagram of Propeller-B performed with a rotation rate of 800 rpm for various turbulator heights.**

While the relative comparisons shed light on the sensitivity, particularly showing a primary impact on thrust, they don't fully address a key concern in the use of propeller turbulence stimulation: What is the isolated impact of this turbulence stimulation? To answer this question, we focus solely on the novel turbulators and disregarded the sand roughness. The reason for this choice is that these experiments offered the highest level of control and the complete boundary layer of the propeller was fully turbulent.

The concept is straightforward. We estimate the propeller efficiency assuming a fully turbulent boundary layer, but without any turbulence stimulation. This involves extrapolating the observed efficiencies at different turbulator heights under the design condition to a hypothetical scenario in which the turbulator height is zero. It's crucial to emphasize that this approach is theoretical, as such a condition in reality would result in a completely laminar boundary layer.

For the design condition J = 0.8, a 2nd order polynomial fit was constructed using least squares, with the resulting curve depicted in Figure 16. This choice of a 2nd order polynomial model was motivated by its simplicity and the exceptionally high goodness-of-fit ($R^2 = 1.0$). When extrapolating efficiency towards lower turbulator heights, the analysis indicates a maximum efficiency at $50\mu m$. Utilizing Equation 4 and Equation 5, the boundary layer thickness $\delta_{99}$ is estimated to be $86\mu m$ at 0.7R indicating that the turbulator is embedded within the boundary layer. However, the nature of the second-order polynomial fit suggests a reduction in efficiency at even lower heights, a prediction that is not physically likely. Consequently, it is presumed that further reduction in turbulator height would not significantly alter the efficiency, as the turbulator would be even more deeply situated in the boundary layer.

The estimated efficiency for a propeller with a fully turbulent boundary layer, without the negative isolated impact of turbulence stimulation, is therefore estimated to be 66.4%. For comparison, the experimentally measured baseline efficiency of 71.3% is also included, corresponding to the propeller without turbulence stimulation and thus exhibiting a partially laminar boundary layer as observed in the propeller paint test, see Figure 11.

When considering the efficiency impact of using $70\mu m$ turbulators, which results in an approximate 0.1% loss, it is clear that this is significantly less severe than the substantial 4.9% efficiency reduction observed when transitioning from a laminar to a turbulent boundary layer. From this, it is evident that the isolated impact of turbulators, particularly at a height of $70\mu m$ and a rotation rate of 800 rpm, on propeller performance is minor. This is especially true when compared to the more substantial effects associated with tripping the propeller boundary layer flow.

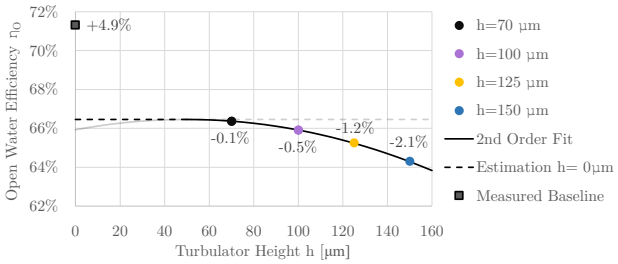


**Figure 16: Estimation of isolated turbulator penalty on the efficiency for Propeller-B for $J = 0.8$ at a rotation rate of 800 rpm ($Re = 7.5 \times 10^5$).**

Analogous to the approach for efficiency, an estimation of the isolated impact on thrust was also conducted following the same procedure. The findings are illustrated in Figure 17. A parallel conclusion to that of the efficiency can be drawn regarding the thrust. Further reduction in the turbulator height is unlikely to significantly affect the thrust of the propeller. Notably, the deviation from the measured baseline is substantial, amounting to a 12.9% relative increase in thrust. This stark contrast underscores the significant influence of the boundary layer regime on propeller thrust.

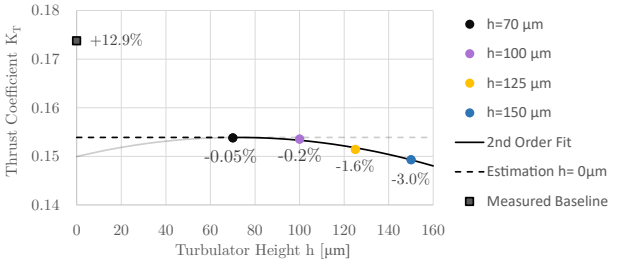


**Figure 17: Estimation of isolated turbulator penalty on the thrust for Propeller-B for $J = 0.8$ at a rotation rate of 800 rpm ($Re = 7.5 \times 10^5$).**

The analysis carried out in this study, which aims to quantify the isolated impact of the turbulators, is as explained above, of a theoretical nature. This is because experimentally inducing boundary layer transition without introducing a loss of momentum is not feasible. However, using CFD, this can be achieved by comparing simulations of fully turbulent flow with those that include transition modelling. The concordance between our experimental observations on propeller performance changes with turbulators and Kerkvliet et al. (2024)'s computational findings substantiates the reliability of our results.

In summary, the systematic variation in height conducted in this study reveals that the isolated impact of turbulence stimulation on propeller performance is rather minimal. Even if this effect had been more pronounced, the resulting penalty due to the parasitic drag of the turbulators would have been very similar across different model propellers. In other words, the application of turbulence stimulation would still enhance the fairness of comparisons between different propeller designs in model testing by mitigating low-Reynolds effects like transition and laminar flow separation.

### 3.5 The Impact of a Turbulent Boundary Layer on Propeller Performance

The preceding sections have established confidence in the boundary layer visualisation technique and demonstrated that the addition of turbulators has a minimal isolated impact on a representative propeller design. Building upon this foundation, the paper now shifts its focus to the core findings, examining the impact of enforcing a turbulent boundary layer on propeller performance.

This section presents a comparative analysis of the open-water performance for three distinct propeller designs, Propeller-B, Propeller-C, and Propeller-D, as detailed in Table 1. The comparison involves evaluating each propeller's baseline performance without turbulence stimulation against its performance including turbulence stimulation. This comparison encompasses both open-water charts and propeller paint test results, offering a comprehensive view of the impacts of turbulence on propeller efficiency.

#### *3.5.1 Propeller-B*

The initial test case employed to illustrate the differences in the boundary layer of propellers involves Propeller-B. Figure 18 displays the open water results for the baseline propeller, comparing it with a propeller that has an optimally distributed leading edge sand roughness and one equipped with 70 $\mu m$ turbulators. An 'optimal distribution' of leading edge sand roughness refers to using three different grit sizes, each selected based on the propeller's radius to effectively trip the boundary layer. This specific sizing was determined through paint tests conducted in a manner similar to the experiments described in the previous section.

The sand roughness distribution applied to the suction side of the propeller was stratified as follows: size L from 0.2789R to 0.6R, size M from 0.6R to 0.8R, and size S from 0.8R to 1.0R. On the pressure side, the distribution was composed of size M from 0.2789R to 0.6R, transitioning to size S from 0.6R to 1.0R.

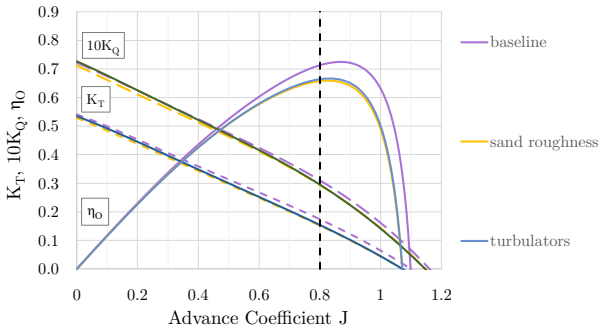


**Figure 18: Open water test results for Propeller-B operating at 800 rpm for the baseline, equipped with an optimal leading edge sand roughness and 70$\mu m$ turbulators.**

As shown in Section 3.4, the use of turbulators reduces the propeller efficiency by 4.9% for the design condition. The sand roughness results in a slightly larger reduction of 5.5%, aligning with literature that suggests sand roughness

is less efficient as it has a larger isolated impact on the propeller performance. Moreover, beyond the efficiency decrease, there is a substantial drop in the thrust coefficient $K_T$ from 0.1737 to 0.1518, amounting to 12.6%. Furthermore, this value is slightly lower than the 0.1538 obtained with the turbulators, resulting a relative reduction of 11.5% with respect to the baseline case. For the sake of clarity, this corresponds to previously reported 12.9% increase in thrust when comparing the propeller fitted with turbulators to the baseline.

Figure 19 illustrates the paint test outcomes for both the baseline propeller and the propeller fitted with turbulators. For the baseline propeller, the results on the suction side depict a fully laminar boundary layer due to the favourable pressure gradient, yet with flow separation occurring near the trailing edge across the entire blade. On the pressure side, the transition to turbulence is observed halfway along the chord, attributable to the adverse pressure gradient, and there is no evidence of flow separation. In contrast, the introduction of turbulators markedly changes these patterns. The paint test results demonstrate successful tripping of the boundary layer on both the suction and pressure sides.

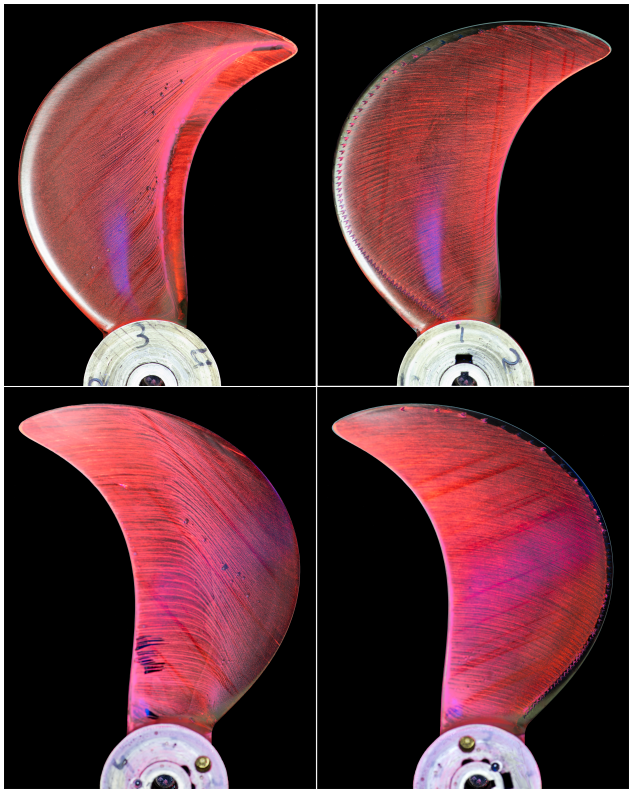

**Figure 19: Comparison of near wall flow patterns for Propeller-B operating at a $J = 0.8$ and a rotation rate of 800 rpm ($Re = 7.5 \times 10^5$). Top: comparison of the suction side between baseline (left) and 70$\mu m$ turbulators (right). Bottom: comparison of the pressure side between baseline (left) and 70$\mu m$ turbulators (right).**

Particularly noteworthy is the strategic positioning of the turbulators, which are placed further down the chord at the lower radii on the suction side. This placement proves especially beneficial for propellers with a high thickness-to-chord ratio near the hub and for wake-adapted propellers, characterized by a reduced pitch near the hub. Such positioning ensures that the turbulators are not located in the stagnation region, therefore maintaining their effectiveness in tripping, even under these specific geometric conditions. To illustrate the improved boundary layer tripping achieved by positioning the turbulators further down the chord, a comparison is presented in Figure 20. When the turbulators are positioned near the leading edge, they fail to trip the boundary layer at the lower radii, leading to laminar separation near the trailing edge.

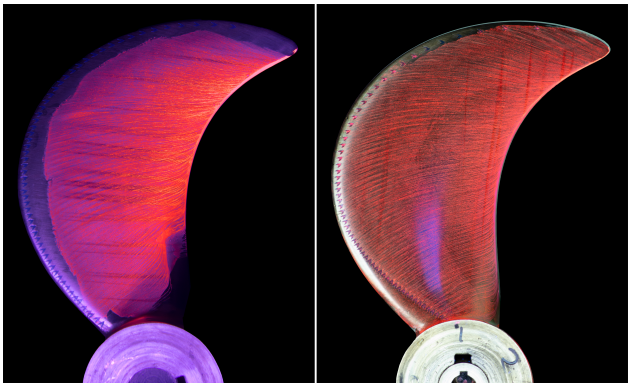

**Figure 20: Comparison of turbulator positions at the lower radii: Near the leading edge (left) and further down the chord (right) for Propeller-B operating at a $J = 0.8$ and a rotation rate of 800 rpm ($Re = 7.5 \times 10^5$).**

Exclusively for Propeller-B, also behind model ship propeller paint tests were conducted to challenge prevalent assumptions in the field. Contrary to various publications demonstrating that the boundary layer of a model propeller is largely laminar during an in-behind model test, there remains a common belief that it becomes largely turbulent due to the turbulence generated by the model ship. To challenge this belief, in-behind paint tests were conducted for Propeller-B using MARIN's reference model ship (Bunt 2023), a model container ship with a scale factor of 33.7. These tests aimed to confirm the presence of a laminar boundary layer. The results, depicted in Figure 21, align with the findings by Tamura and Sasajima (1977), Lücke and Streckwall (2017), and Hasuike et al. (2018), indicating that the boundary layer remains fully laminar when the propeller operates behind a ship model.

A significant difference in trailing edge flow separation, as can be seen in Figures 21, was also observed. As Li et al. (2019) concluded, accurately determining the relative rotative efficiency becomes significantly more complicated when substantial flow separation occurs during the POT but not during the propulsion test. Since relative rotative efficiency is typically assumed constant during extrapolation, this inconsistency at the model scale can substantially affect the final prediction of ship performance. However, it is important to note that operating behind a ship model subjects the propeller to varying inflow, resulting in different angles of attack, and consequently, the point of flow separation varies due to dynamic blade loading. Therefore, while a steady POT may reveal a clear separation point,

identifying this becomes virtually impossible for a behind ship model paint test.

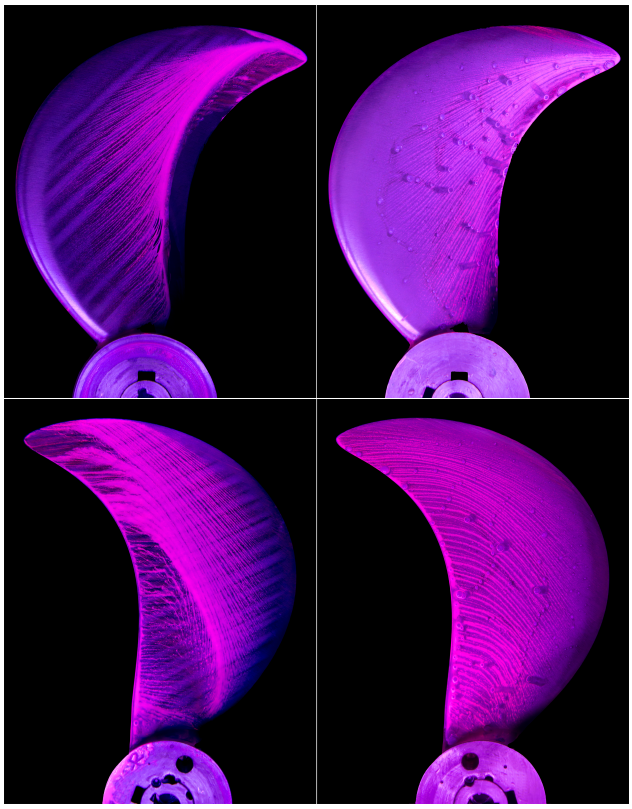

**Figure 21: Comparison of near wall flow patterns for baseline Propeller-B operating at a $J = 0.745$ and a rotation rate of 400 rpm ($Re = 3.7 \times 10^5$). Top: comparison of the suction side between open-water (left) and propulsion test (right). Bottom: comparison of the pressure side between open-water (left) and propulsion (right).**

### *3.5.2 Propeller-C*

Figure 22 displays the open water results for Propeller-C, capturing both high and low Reynolds number scenarios. For high Reynolds numbers, rotation rates ranged from 475 to 800 rpm, while at low Reynolds numbers, the rotation rate was consistently held at 500 rpm. The torque limitation of 100 Nm by the dynamometer, as outlined in Section 2.4, restricted the exploration of higher Reynolds numbers. The characteristics of Propeller-C are detailed in Table 1. This propeller was chosen as it markedly accentuates the differences between laminar and turbulent boundary layers caused by its small blade area. For the baseline open water results, a distinct dip is observed in the $10K_Q$ curve, and a more subtle variation is noted in the $K_T$, between advance coefficients of 0.2 and 1.0.

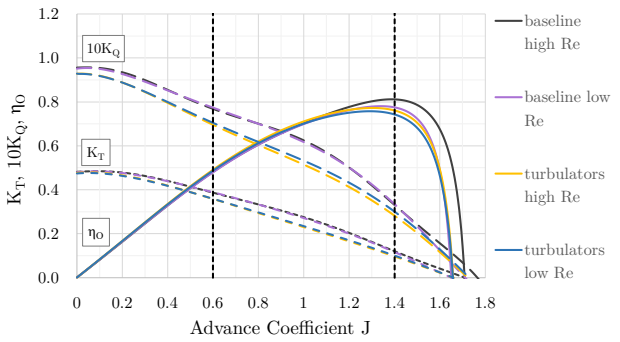


**Figure 22: Open water test results for Propeller-C baseline and $100\mu m$ turbulators.**

For the high advance coefficient, the propeller exhibits laminar flow on both the suction and pressure sides, as shown in Figure 23. However, at a reduced advance coefficient, the leading edge vortex on the suction side induces a turbulent boundary layer. This transition significantly decreases the section's lift, leading to reduced thrust and torque. When turbulators are fitted onto the propeller, a turbulent boundary layer is established on both sides instead of only the suction side, causing a further decrease in thrust and torque.

In examining the maximum open water efficiency, it is observed that the disparity between low and high Reynolds number cases becomes less marked when the propeller is fitted with turbulators. The small difference that is present can be attributed to the Reynolds scaling effects. In stark contrast, the baseline cases (without turbulators) demonstrate significant deviations, primarily caused by a deviation in the laminar trailing edge separation.

It is also interesting that for Propeller-C, turbulence stimulation results in a larger effect on $K_Q$ than on the $K_T$, which was not the case for Propeller-B. An additional point of interest concerning this propeller is the relatively larger difference in torque coefficient $K_Q$ at an advance coefficient J of 0 between the baseline and the turbulators. This also contrasts with Propeller-B, as depicted in Figure 18, where the discrepancy between the baseline and propeller equipped with turbulators is minimal. This difference may be linked to the flow separation region observed at the lower radii on the pressure side of the baseline propeller. Notably, this separation region is mitigated upon the application of turbulators, underscoring their effectiveness in altering flow characteristics.

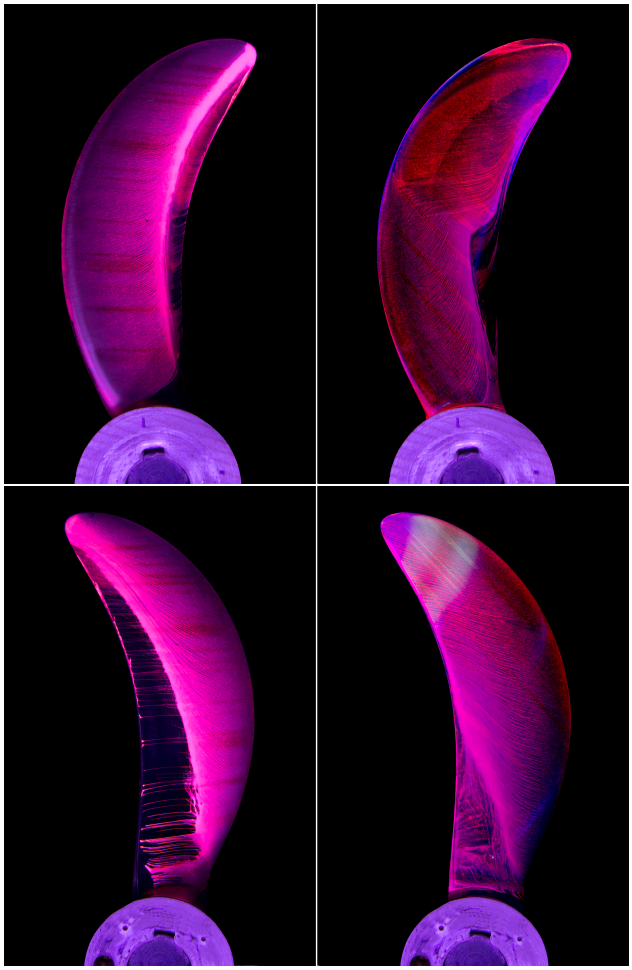

**Figure 23: Paint test results of Proceller-C operating at 800 rpm without turbulence stimulation, for advance coefficients $J = 1.4$ ($Re = 4.9 \times 10^5$) (left) and $J = 0.6$ ($Re = 4.3 \times 10^5$) (right). The top images show the suction side of the propeller, while the bottom images depict the pressure side.**

### *3.5.3 Propeller-D*

The final test-case propeller is a variant characterized by a high blade area ratio as detailed in Table 1. The open water results for the baseline and the propeller with turbulators for a high and low Reynolds number are presented in Figure 24. For the high Reynolds number tests, the rotation rate varied between 800 and 1400 rpm. In contrast, for the low Reynolds number tests, the rotation rate was kept constant at 500 rpm.

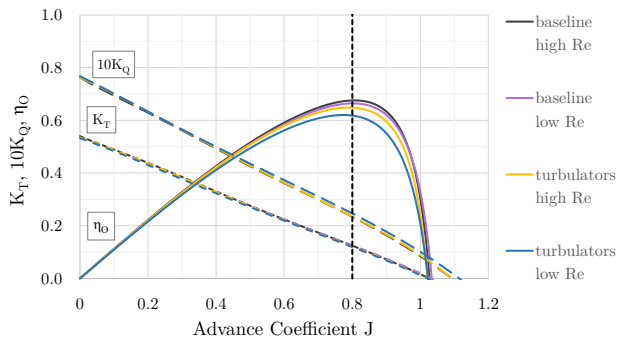


**Figure 24: Open water test results for Propeller-D baseline and 100$\mu$m turbulators.**

The efficiency differences between high and low Reynolds numbers for the baseline Propeller-D are small, in contrast to Propeller-C. This small difference can be explained by Figure 25. At low Reynolds numbers, laminar flow separation occurs at the lower radii, but this separation diminishes as the Reynolds number increases, thereby enhancing propeller performance. The reduction in the extent of laminar flow separation is attributed to the onset of transition at higher Reynolds numbers, caused by the large blade area of the propeller. This formation of a partially turbulent boundary layer on its turn negatively impacts propeller performance. Consequently, the generally positive effects of a higher Reynolds number and the reduction of trailing edge separation are somewhat offset by an earlier transition to a turbulent boundary layer. This dynamic interplay explains why these types of propellers exhibit fewer anomalies in propulsion factor trends, although their boundary layer flow is drastically different between low and high Reynolds numbers.

When comparing the baseline performance at a high Reynolds number of $1.8 \times 10^6$ to that of the propeller equipped with turbulators, an approximate 4% reduction in efficiency is observed. This reduction is primarily due to to a 3.7% decrease in $K_T$ and a slight 0.4% increase in $K_Q$. Despite the high Reynolds number, a notable performance difference persists. This is attributed to the presence of a significant laminar boundary layer region on the suction side of the baseline propeller, as evidenced in Figure 25.

Comparing the low and high Reynolds number of the propeller with turbulators, a relative large difference is found in comparison to Propeller-C. This difference is only caused by a difference in Reynolds number and not by low-Reynolds scale effects such as transition and flow separation. The reason that it is relatively large, is that the boundary layer has a great influence on a propeller with a large blade area.



**Figure 25: Paint test results of Proceller-D operating at $J = 0.8$ for 400 rpm ($Re = 6.0 \times 10^5$) (left) and 1200 rpm ($Re = 1.8 \times 10^6$) (right). The top images show the suction side of the propeller, while the bottom images depict the pressure side.**

## 4 CONCLUSIONS AND RECOMMENDATIONS

This research has comprehensively investigated the boundary layer behaviour of model propellers and the efficacy of turbulence stimulation techniques. Aiming to refine the precision of propeller model testing, it addresses low-Reynolds scale effects, with as overarching long-term aim to improve full-scale performance predictions. The principal findings of this study are summarised as follows.

Firstly, the paint-based boundary layer visualisation technique employed in this study is validated as an effective method for analysing boundary layer flow characteristics on model propellers. We underscore critical aspects regarding the interpretation of paint test results and the assessment of propeller force convergence, essential for ensuring test reliability. This foundational achievement underpins the subsequent findings.

The enhanced paint tests show that at Reynolds numbers typical for model propellers, the boundary layer tends to remain laminar or partially laminar across the entire range of typical model test Reynolds numbers. This poses considerable challenges for the accuracy, interpretability, and reliability of model tests, and their extrapolation to full-scale applications.

Previous studies have proposed using CFD to correct for these low-Reynolds number challenges, as introducing turbulence stimulation during model tests for propellers has been found to be excessively challenging. Two primary concerns have been identified: the inability to distinguish the effects of realising a turbulent boundary layer from the isolated impact of the turbulence stimulation needed and the inadequacy of currently used empirical scaling procedures.

In promoting industry acceptance of propeller turbulence stimulation in model tests, this study addressed the gap in quantifying the isolated impact by systematically varying the turbulence stimulation height and ensuring a completely tripped propeller boundary layer. Not only did this research quantify the isolated impact of turbulence stimulation, but it also introduced a highly efficient type referred to as turbulators with minimal isolated impact on propeller performance. The results indicate that turbulators alone accounted for efficiency changes ranging from 0.1% to 0.6%, while the transition from a laminar to a turbulent boundary layer resulted in a 4.9% efficiency change. The isolated impact of the turbulators on thrust was even smaller, amounting to approximately 0.2%, whereas the difference due to boundary layer changes led to a 12.9 % reduction. Hence, the isolated impact of the turbulators on propeller performance is relatively minor. Furthermore, these innovative turbulators are practical and consistent compared to traditional sand roughness.

Detailed comparisons across three distinct propeller types were performed, focusing on the performance disparities between tests using the newly developed turbulators and the conventional tests without turbulence stimulation. This analysis revealed that propellers with a lower blade area are particularly sensitive to Reynolds number effects on efficiency in the absence of turbulence stimulation. At typical model-scale Reynolds numbers, these propellers often exhibit a predominantly laminar boundary layer, leading to flow separation at the trailing edge. A clear trend was observed in these propellers, where an increase in Reynolds number resulted in higher propeller efficiency. Conversely, for propellers with larger blade areas, the absence of turbulence stimulation led to less pronounced differences. This was attributed to the counterbalancing effects of the higher Reynolds number's generally positive impact and the reduced trailing edge separation, weighed against the earlier onset of a turbulent boundary layer.

Additionally, it was observed that operational conditions also influence the boundary layer regime. Even for propellers with a small blade area, which are fully laminar under design conditions, boundary layer transition can occur at higher loading conditions. This transition is triggered by the leading edge vortex, leading to a flow separation-induced transition.

The use of turbulators reduces the effects of boundary layer transition and laminar separation on propeller efficiency variations with Reynolds number. This results in more consistent performance trends across different propeller types. Such findings highlight the importance of turbulators in improving the consistency of model testing and allowing a more equitable comparison between different propeller designs through model testing.

Another critical finding of this study is the optimised positioning of turbulators further down the chord at lower radii on the suction side of the propeller blades, strategically avoiding their placement in the stagnation region. This positioning proves especially effective for propellers with high thickness-to-chord ratios at these radii. It is also advantageous for wake-adapted propellers with a reduced

pitch near the hub.

The next step is to revise the current scaling procedures, such as the ITTC-78, by developing CFD-based extrapolation methods. This approach is expected to reflect the effects of Reynolds scaling more accurately, bridging the gap between model-scale tests and full-scale propeller performance.

In summary, this research significantly advances our understanding of the boundary layer behaviour for model propellers and introduces an innovative turbulator design. These findings are critical to improving the accuracy of model testing, better matching experimental results with CFD simulations, enabling more accurate full-scale predictions through CFD-based extrapolation, and ultimately contributing to more efficient marine propulsion systems.


## ACKNOWLEDGEMENTS

This research was partly funded by the Dutch Ministry of Economic Affairs.

We express our deepest gratitude to Gert Kuiper, Do Ligtelijn and Martin Hoekstra for their invaluable guidance and insights throughout this research. Their expertise has significantly shaped the direction and execution of this study. Their contributions post-retirement have been both remarkable and deeply appreciated.

Additionally, we extend our thanks to our colleagues Johan Bosschers, João Baltazar, Jie Dang, John Huisman, Harm Jan Kamphof, Martijn van Rijsbergen, Michiel Verhulst, Christiaan Pouw and Tom van Terwisga for their thoughtful discussions and encouragement.

In conclusion, special thanks are due to Twan Peters, Emiel Seves, Henk Roest, Kristan van Roekel, Michael Stahlhoff, Anthony Kasdjo and Jeroen Bosch. This paper could not have been made without their experimental expertise and their exceptional commitment to going above and beyond in their contributions to our work.


## REFERENCES


Aucher, M., Bowden, B.S., Gross, A., Lindgren, H., Minsaas, K.J., Muntjewerf, J.J., Tamura, K., Wermter, R. (1978). 'Report of Performance Committee'. 15 th International Towing Tank Conference, ITTC, The Hague, The Netherlands

Allan, J.F., Couch, R.B., Lerbs, H.W.E., Telfer, E.V. (1951). 'Subject 1 - Reynolds Number for Model Propeller Experiments'. 6th International Conference of Ship Tank Superintendents, ITTC, Washington, United States of America

Baltazar, J., Rijpkema, D. & Falcão de Campos, J. (2018). 'On the use of the $\gamma - Re_{\theta_t}$ transition model for the prediction of the propeller performance at model-scale', Ocean Engineering **170**, pp. 6–19.

Baltazar, J., Schuiling, B. & Kerkvliet, M. (2023). 'Modelling of Laminar-to-Turbulent Flow Transition on a Marine Propeller Using a RANS Solver', 25th Numerical Towing Tank Symposium, Ericeira, Portugal.

Bhattacharyya, A., Neitzel, J.C., Steen, S., Abdel-Maksoud, M., Krasilnikov, V. (2015). 'Influence of Flow Transition on Open and Ducted Propeller Characteristics'. Fourth International Symposium on Marine Propulsors, Austin, United States of America

Boorsma, A. (2000). 'Improving full scale ship powering performance predictions by application of propeller leading edge roughness'. Master of Science Thesis, University of Technology, Delft, The Netherlands

Braslow, A.L & Knox, E.C. (1958). 'Simplified method for determination of critical height of distributed toughness particles for boundary-layer transition at mach numbers form 0 to 5', NACA technical note 4363, USA

Bunt E. van de, Tukker J., Rijsbergen M. van, Pouw, C. and Dekker J. (2023). 'Evaluating Experimental and Analysis Uncertainty in Resistance Testing', 7th International Conference on Advanced Model Measurement Technology for the Maritime Industry (AMT'23), Istanbul, Turkiye

Elsinga, G.E. & Westerweel, J. (2012). 'Tomographic-PIV measurement of the flow around a zigzag boundary layer trip'. Experiments in Fluids **52**, 865–876.

Gutsche, F. (1936). 'Kennwerteinflusse bei Schiffsschrauben-Modellversuchen'. Preusz. Versuchsanstalt fur & Wasserbau und Schiffbau **21**, Berlin, Germany.

Gutsche, F. (1940). 'Versuche an umlaufenden Flügelschnitten mit abgerissener Strömung'. Jahrbuch der Schiffbautechnischen Gesellschaft Vol **41**, pp. 188-226, Berlin, Germany.

Hasuike, N, Okazaki, M, Okazaki, A. & Fujiyama, K. (2017). 'Scale effects of marine propellers in POT and self propulsion test conditions'. 5th International Symposium on Marine Propulsors, Espoo, Finland.

Hughes, G & Allan, J.F. (1951). 'Turbulence Stimulation on Ship Models'. Transactions of Society of Naval Architects & Marine Engineers **59**, pp. 281-314

ITTC (2002). 'Testing and Extrapolation Methods Propulsion, Propulsor Open Water Test'. Recommended Procedures and Guidelines, 7.5-02-03-02.1

ITTC (2017). '1978 Powering Prediction Method'. Recommended Procedures and Guidelines, 7.5-02-03-01.4

Kerkvliet, M., Baltazar, J., Schuiling, B. & Eça, L. (2024). 'A Numerical Study on Model Propeller Performance Prediction Including Transitional and Passively Controlled Boundary Layer Considerations', 8th International Symposium on Marine Propulsors, Berlin, Germany.

Kuiper, G. (1978). 'Scale Effects on Propeller Cavitation Inception (1978)'. Proceedings of the 12th Symposium on Naval Hydrodynamics, Office of Naval Research, Washington D.C., United States of America.

Kuiper, G. (1981). 'Cavitation Inception on Ship Propeller

Models'. PhD. Thesis, Delft, The Netherlands.

Lammeren W.P.A. van (1939). 'Propulsion Scale Effects'. North East Coast Institution of Engineers and Shipbuilders , Volume **56**, pp. 115-152, London, The United Kingdom.

Li, D-Q., Lindell, P. & Werner S. (2019) 'Transitional Flow on Model Propellers and Their Influence on Relative Rotative Efficiency'. Journal of Marine Science and Engineering, **7**(12):427.

Lücke, T. & Streckwall, H. (2017) 'Experience with Small Blade Area Propeller Performance'. 5th International Symposium on Marine Propulsors, Espoo, Finland.

Lücke, T (2019) 'Particular Model Propeller Behavior in EFD & CFD'. 6th International Symposium on Marine Propulsors, Rome, Italy.

Lyon, C.A., Selig, M.S. & Broeren .A.P. (1997). 'Boundary layer trips on airfoils at low Reynolds number'. 35 th AIAA Aerospace Sciences Meeting and Exhibit, Reno, NV, USA, AIAA-97-0511.

Meyne, K. (1972). 'Untersuchung der Propellergrenzschichsströmung under der Einfluß der Reibung auf der Propellerkenngrößen.'. Jahrbuch der Schiffbautechnischen Gesellschaft **66**, pp. 317-402, Hamburg, Germany.

Rooij, R.P.J.O.M. Van, Timmer, W.A. (2003). 'Roughness sensitivity considerations for thick rotor blade airfoils', Journal of Solar Energy Engineering **125**, pp. 468–478

Rijpkema, D., Baltazar, J. & Falcão de Campos, J. (2015). 'Viscous flow simulations of propellers in different Reynolds number regimes'. Proceedings of the Fouth International Symposium on Marine Propulsors, SMP'15, Austin, Texas, USA.

Salvant Plisson, J., de Viguerie, L., Tahroucht, L., Menu, M., Ducouret., G. (2014). 'Rheology of white paints: How Van Gogh achieved his famous impasto'. Colloids and Surfaces A: Physicochemical and Engineering Aspects, Elsevier, 458,pp. 134-141.

Streckwall, H, Greitsch, L, Müller, J., Scharf, M. & Bugalski, T. (2013). 'Development of a Strip Method Proposed as New Standard for Propeller Performance Scaling'. Ship Technology Research, 60:2, 58-69

Tamura, K. & Sasajima, T. (1977) 'Some Investigations on Propeller Open-Water Characteristics for Analysis of Self-Propulsion Factors'. Mitsubishi Technical Bulletin **66**, Mitsubishi Heavy Industries Ltd., Tokyo, Japan.

Tanibayashi, H., Bailey, D. , van Berlekom, W., Collatz, G., Della Loggia, B., Holtrop, J., Ikehata, M., McCarthy, H., Varsamov, K. (1987). 'Report of Powering Performance Committee'. 18 th International Towing Tank Conference, ITTC, Kobe, Japan.

Wheeler, G.O. (1991). 'Low Drag Vortex Generators'. US Patent 5,058,837,filed April 7, 1989, and issued October 22, 1991

White, F. (2010). Fluid Mechanics. 7th ed. Mcgraw-Hill Book Company.